*17th World Conference on Earthquake Engineering, 17WCEE*
*Sendai, Japan - September 13th to 18th 2020*

# A VECTOR-VALUED INTENSITY MEASURE FOR THE SEISMIC RESPONSE ASSESSMENT OF STRUCTURES IN NEAR-FAULT REGION

E. Zengin[(1)], N.A. Abrahamson[(2)]

[(1)] *Visiting Scholar, University of California, Berkeley, esrazengin@gmail.com*
[(2)] *Adjunct Professor, University of California, Berkeley, abrahamson@berkeley.edu*

## Abstract

The forward-directivity ground motions produce large amplitude and high-energy velocity pulses that may cause severe damage to structures. The amplitude and frequency content of the pulse-like ground motions have been generally characterized by peak ground velocity and pulse period. These motions have a peaked spectral shape around the pulse period. The most commonly used ground-motion intensity measure (IM), i.e., the 5% damped elastic spectral acceleration at the fundamental period of the structure ($Sa(T_1)$) is insufficient to capture the effects of velocity pulses on structural response. Using spectrally equivalent pulse-like and non-pulse-like record pairs, we test whether the damaging effects of the near-fault ground motions are adequately captured by the velocity pulse parameters and find that they are not. We introduce a period-dependent ground-motion parameter, Instantaneous Power ($IP(T_1)$), which is defined as the maximum rate of change of energy of the bandpass filtered velocity time series over a short time interval. The velocity time series is bandpass filtered between $0.2T_1$ and $3T_1$, hence the $IP(T_1)$ takes into account the frequency content of the ground motion that can excite the structure. The $IP(T_1)$ is intended to supplement the $Sa(T_1)$ in the prediction of the response of structures subjected to near-fault ground motions. We find that the proposed vector-valued IM [$Sa(T_1)$, $IP(T_1)$] reduces the record-to-record variability in peak displacement-based structural responses better than the velocity pulse parameterization and fully accounts for the pulse-period effect. A new conditional ground-motion model has been developed for the $IP(T_1)$. We demonstrate that the vector IM leads to a more reliable probabilistic seismic risk assessment of structures. In the context of record selection, the use of the $IP(T_1)$ would circumvent the need for explicit consideration of the velocity pulse and pulse period.

*Keywords: near-fault ground motion; pulse; vector intensity measure; record selection; seismic risk*

## 1. Introduction

The seismic performance of structures located in the near-fault region may be adversely affected by the ground motions containing velocity pulses. A fault rupture propagating toward a site with a velocity close to the shear wave velocity leads to constructive interference of the waves, which causes large energy pulses in a short period of time. This phenomenon, also known as forward directivity, results in intense pulse in the velocity time series as well as a peculiar spectral shape around the period of the pulse ($T_p$). The average spectral amplitudes of the pulse-like ground motions (around the $T_p$) are systematically higher than that of the far-field ground motions, imposing a higher demand on the structure. Therefore, understanding the effect of velocity pulses on structural response and characterizing the damage potential of the near-fault ground motions are critical for the reliable seismic design and assessment of structures.

Within the context of performance-based seismic assessment and design, one of the major tasks is the estimation of the probabilistic structural response due to future earthquakes at the given site. An intensity measure (IM) is typically used to characterize the earthquake shaking as well as the corresponding relationship between the structural response and probabilistic seismic hazard analysis (PSHA). The reliable and accurate estimation of the structural performance depends on the ability of an IM to capture the characteristics of the ground motion that affect the structural response. It is desirable to have an IM that reduces the dispersion in the structural response (ie., efficiency) and renders the conditional distribution of structural response independent of other ground motion characteristics (ie, sufficiency). The 5% damped elastic spectral acceleration at the fundamental period of the structure ($Sa(T_1)$) is widely used in performance-based earthquake engineering. Although the $Sa(T_1)$ is found to be an efficient IM in predicting the response of a first-mode dominated structure, it does not account for the effects of higher modes and inelastic structural response. Baker and Cornell [1] demonstrated that the vector IM consisting of $Sa(T_1)$ and epsilon ($\varepsilon$), ie. number of standard deviations of spectral ordinates of the as-recorded ground motions from the median predictions obtained from ground-motion model, improves the structural response predictions for far-field ground motions. However, severe responses occurred due to the near-fault ground motions are not well captured by the $Sa(T_1)$ or [$Sa(T_1)$, $\varepsilon$]. In particular, the aforementioned IMs are found to be insufficient with respect to the ratio of the pulse period to the fundamental period of the structure ($T_p/T_1$), which is considered as the key parameter affecting the structural response. In this case, the distribution of structural response would depend on the type of records utilized in the analysis. Several advanced and vector-valued IMs motions have been proposed to account for the effects of pulse period [2-5]. For instance, Luco and Cornell [4] proposed an advanced IM, which combines the effects of higher modes and inelastic structural response. Baker and Cornell [5] proposed a vector-valued IM containing $Sa(T_1)$ and the ratio of the spectral acceleration at period $T_2$ to the first-mode period of the structure ($R_{T1,T2}$), which accounts for the effects of spectral shape.

This study proposes a new vector-valued intensity measure, consisting of $Sa(T_1)$ and Instantaneous Power ($IP(T_1)$), to better characterize the destructive potential of the near-fault ground motions. The $IP(T_1)$ is defined as the maximum energy rate of the bandpass filtered velocity time series over a short time interval. The velocity time history is bandpass filtered between $0.2T_1$ and $3T_1$, so that the frequencies that are relevant to the structural response are considered. Using two-dimensional models of the 2- and 9-story steel-frame buildings, we evaluate the efficiency and sufficiency of the proposed [$Sa(T_1)$, $IP(T_1)$] vector IM in predicting the drift-based responses and compare the results with those obtained using the velocity pulse parameters. We develop a new conditional ground-motion model for the $IP(T_1)$ which is based on $Sa(T_1)$, magnitude(M), and rupture distance ($R_{rup}$). The seismic drift hazard curves obtained with the vector IM are compared with those based on $Sa(T_1)$ scalar IM. We briefly discuss how the conditional ground-motion model can be used to select near fault-ground motions for seismic response analysis.



 

## 2. Instantaneous Power

To increase the efficiency and the sufficiency of the $Sa(T_1)$, a new period-dependent ground-motion parameter, $IP(T_1)$ was proposed [6]. It was found that the cumulative energy-based IMs (e.g., Arias Intensity, root mean square acceleration) are not capable of reducing the dispersion in the peak displacement-based responses for a given $Sa(T_1)$. We observed that the $IP(T_1)$ better predicts the structural response than the existing IMs. The $IP(T_1)$ represents the maximum rate of change of energy of the bandpass filtered velocity time history over a short period of time. In the filtering process, a four-pole Butterworth bandpass filter in the frequency domain for the $[0.2T_1\text{-}3T_1]$ period range is used. The power of the filtered velocity time history is calculated over a sliding window of one half of the fundamental period of the structure (i.e., $[t, t+0.5T_1]$).

The $IP(T_1)$ is given by

$$IP(T_1) = max\left(\frac{1}{\Delta t}\int_{t}^{t+\Delta t} V^2{}_{filtered}\ (\tau)d\tau\right) \tag{1}$$

where IP is in units of in $cm^2/s^2$, $V_{filtered}(\tau)$ is the bandpass-filtered velocity of the record in cm/s, and $\Delta t$ corresponds to $0.5T_1$. Fig. 1A shows an example of an original and filtered velocity time histories of a pulse-like record for $T_1$=1.0 s. For this case, the passband for the filtering is 0.2 seconds to 3.0 seconds. Fig. 1B shows the variation of the velocity power of the filtered time series over the time interval $0.5T_1$ (i.e., 0.5 sec). The $IP(T_1)$ of the record corresponds to the maximum value of 1440 ($cm^2/s^2$).

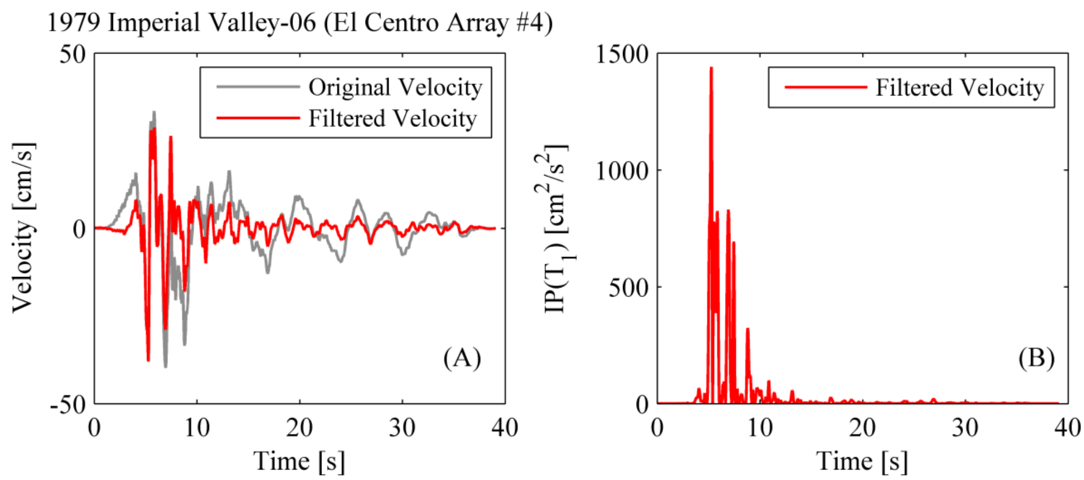


Fig. 1 – (A) Illustration of the original and filtered velocity time histories of the selected pulse-like record (1979 Imperial Valley-06 earthquake recorded in the El Centro Array #4 station) for $T_1$=1.0 s. The bandpass for the filtering is 0.2 seconds to 3.0 seconds. (B) Time variation of the instantaneous power of the filtered time history [6].

The $IP(T_1)$ captures the key features of the velocity pulses in the relative amplitude of the ground motion. The left panel in Fig.2 shows the residuals of PSA(T=2s) for near-fault ground motions using the PEER NGA-W2 data set. The recordings classified as having a velocity pulse are shown by the red symbols. At short distances (less than 10 km), the pulse records have systematically larger PSA than the records without a pulse. The right panel in Fig. 2 shows the residuals of the sqrt(IP(T=2s)) for the same data set. The near-fault recordings with pulses tend to have larger IP than the records without a pulse. This indicates that the $IP(T_1)$ is capturing the amplitude information in the pulse recordings.

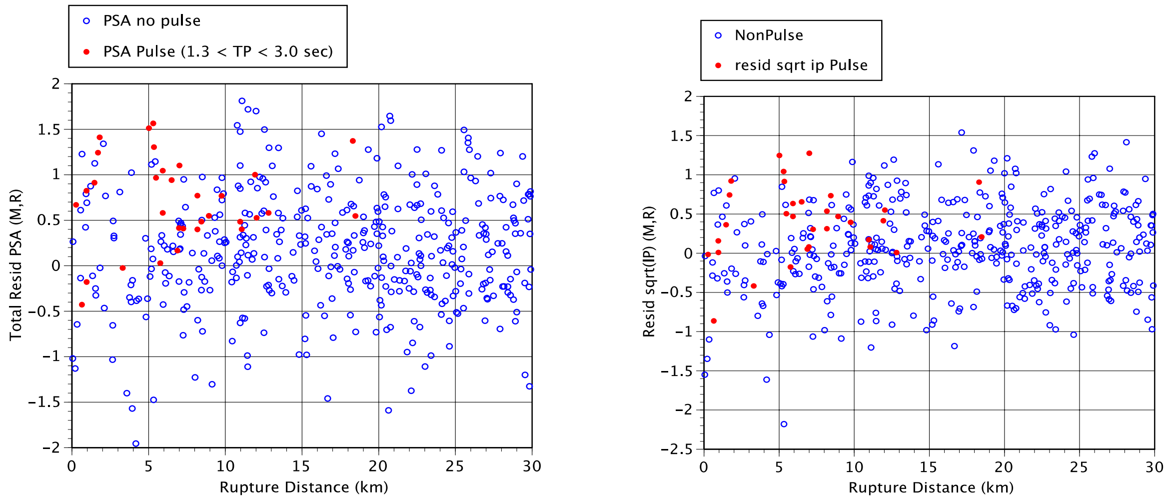


Fig. 2 – The residuals of the PSA(T=2s) in the left figure show that the pulse records tend to have larger than average PSA(T=2). The residuals for Sqrt(IP(T=2s)) in the right figure show that the pulse records have above average IP in addition to above average PSA.

## 3. Selection of Spectrally Equivalent Pulse-like and Non-pulse-like Records

The subsets of near-fault pulse-like and non-pulse-like records used in this study are selected from Pacific Earthquake Engineering Research Center (PEER) Strong Motion Database. The records are selected in the magnitude range 5.5-8.5 and the rupture distance range 0-30 km. The pulse-like records and their periods are identified using the wavelet transformation method proposed by Shahi and Baker [7]. The $T_p$ values of the pulse-like record are selected within the $[0.5T_1\text{-}3T_1]$ period range in order to consider the pulses that are relevant to the response of the structure. It is well known that the peculiar spectral shape of the pulse-like record is one of the key characteristics of the ground motion affecting the structural response. To investigate the effect of the time-domain characteristics of the ground motion on the structural response, we eliminate the effect of spectral shape by employing spectrally equivalent pulse-like and non-pulse-like record pairs. We perform all pairwise comparisons between the scaled response spectra of the non-pulse-like records and target response spectra of the pulse-like records. A scale factor (sf) is calculated by averaging the spectral values of the pulse-like and non-pulse-like record spectra over a period range of $[0.2T_1\text{-}3T_1]$, and then taking the ratio of these values. The non-pulse-like records with sf greater than 5 are eliminated. The mismatches between the response spectra of the record pairs are evaluated by using the sum of squared error (SSE) metric, which can be computed as follows:

$$SSE = \sum_{i=1}^{n}[\ln Sa_P(T_i) - \ln(sf\ Sa_{NP}(T_i))]^2 \tag{2}$$

where $\ln Sa_P(T_i)$ is the logarithmic spectral ordinates of the pulse-like record spectrum at period $T_i$, and $\ln Sa_{NP}(T_i)$ is the logarithmic spectral ordinates of the non-pulse-like record spectrum at period $T_i$. The record pairs that had the smallest SSE values are used as input to the nonlinear dynamic analysis. The detailed information about the record selection approach can be found in Zengin et al. [8]. For illustration purposes, we show the velocity time histories of the scaled non-pulse-like (2009 L'Aquila Italy Earthquake) and the original pulse-like (1995 Kobe Japan Earthquake) record pair in Fig. 3A. These records are selected for $T_1$=2.2 seconds. Fig. 3B illustrates a comparison of the response spectra of the spectrally equivalent record pairs. Although not shown here, we found that the response spectra of the pulse-like and non-pulse-like record sets have similar median and dispersion values within the specified period range (ie, $0.2T_1\text{-}3T_1$).



 

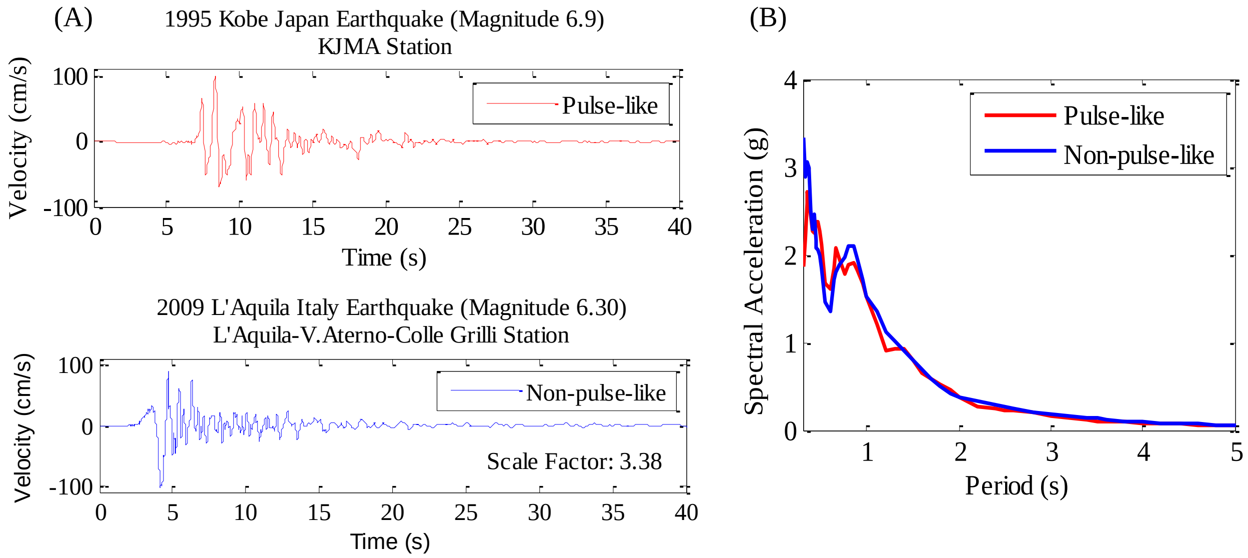


Fig. 3 – Comparison of (A) velocity time histories and (B) response spectra of the spectrally equivalent pulse-like and non-pulse-like record pair.

## 4. Building Information

The effectiveness of the proposed IM is evaluated by analyzing the 2- and 9-story steel-frame buildings that were designed in accordance with the UBC 1988 with State of California amendments and the provisions of 2001 California Building Code, respectively. The 2-story steel frame building is located in Fremont, California and the 9-story steel frame building is located in Los Angeles, California. Two-dimensional analytical models of the buildings are constructed in the OpenSees platform. The concentrated plastic hinge elements are used for the beam and column members, and the Modified Ibarra Krawinkler (ModIMK) deterioration material model, which accounts for the stiffness and strength deterioration, is adopted to model the behavior of the plastic hinges. The parameters of this material model are computed using the empirical equations proposed by Lignos [9]. To account for the P-Delta effects caused by interior frames, the equivalent-gravity frame is constructed and linked to the resisting frame with axially rigid truss elements. The fundamental periods of the 2- and 9-story steel frame structures obtained from eigenvalue analyses are 0.55 and 2.20 seconds, respectively.

## 5. Significance of Pulse Period on Structural Response

This section investigates whether the pulse-like and non-pulse-like record set produce similar structural responses, ie. maximum interstory drift ratio (MIDR), after eliminating the effects of the spectral shape and amplitude. Nonlinear dynamic analyses of the steel frame structures are performed using the subsets 40 spectrally equivalent pulse-like and non-pulse-like records. The records are then scaled to the target Sa($T_1$) level, representing the 2% exceedance in 50 years (denoted as 2/50). The target Sa($T_1$) levels for the 2- and 9-story steel frame structures are 2.05g and 0.3g, respectively. Fig. 4 shows the cumulative distribution function (CDF) of the drift responses for both structures. It is seen that the pulse-like records produce higher median drift responses than the non-pulse-like records. The velocity pulses have a more pronounced effect on the response of 2-story structure. Moreover, pulse-like record sets produce higher dispersion in the structural responses for both cases. These results suggest that the consideration of the spectral shape is not adequate to characterize the damage potential of the velocity pulses. In other words, there are still uncontrolled factors in time-histories affecting the structural response.



 

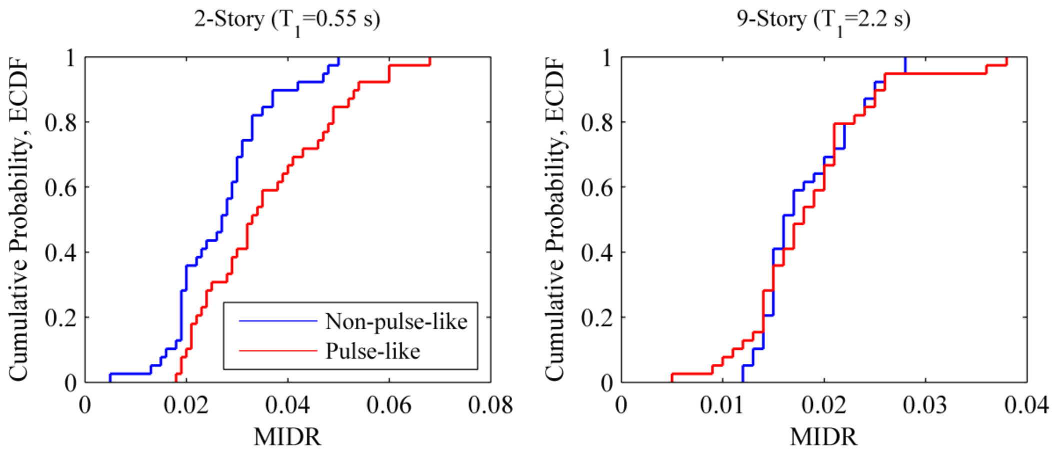


Fig. 4 – Empirical cumulative distribution functions (ECDFs) of the MIDRs for the 2- and 9-story steel-frame structures, under the spectrally-equivalent pulse-like and non-pulse-like record sets [6].

Previous studies showed that the structural response is sensitive to the $T_P/T_1$ parameter. For example, the records with $T_P/T_1>2$ are classified as "aggressive", whereas the records with $T_P/T_1<2$ are labelled as benign. The aggressive behavior of the velocity pulse indicates that the pulse-like record is more damaging than the non-pulse-like record, whereas benign refers to the less damaging behavior of the pulse-like record. To investigate whether the $T_p/T_1$ is a good predictor of the structural response, we plot the relationship between $T_p/T_1$ and MIDR in Fig. 5. The coefficient of determination ($R^2$), which is the proportion of the variance in the dependent variable that can be explained by the independent variable, is used to assess the effect size. The effect sizes based on Cohen's criteria [10] are: $R^2$=0.01 is a weak correlation effect; $R^2$=0.09 is a moderate correlation effect; and $R^2$=0.25 is a large correlation effect. As seen in Fig. 5, the $T_p/T_1$ has a moderate effect on the drift response of 2-story structure. In this case, the larger $T_p/T_1$ ratios partly explain the higher drift responses of 2-story structure. For the 9-story steel structure, the lack of correlation between $T_p/T_1$ and MIDR likely suggests that the differences in structural response are not about the $T_p$ but about other characteristics of the pulse-records.

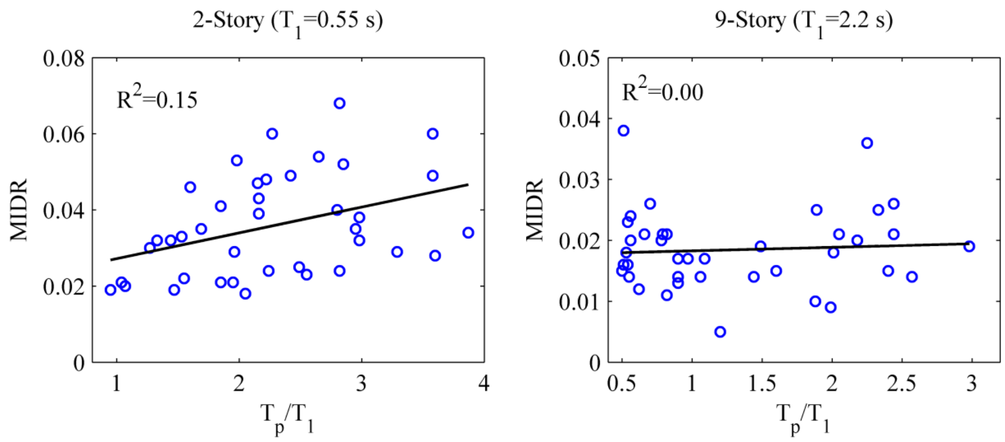


Fig. 5 – Relationships between MIDRs and the distributions of $T_p/T_1$ for the 2- and 9-story steel-frame structures [6].

We further investigate the dependency of the median drift responses on $T_p/T_1$. Fig. 6 illustrates the moving averages of 4 responses obtained from the pulse-like records. The moving average window approach allows us to examine how the responses change in smaller $T_p/T_1$ bins. The average drift responses for non-pulse-like records are also shown (horizontal lines) in Fig. 6, for comparison. The deviation of the moving average curve from the horizontal line can be used to evaluate the aggressive (or benign) behavior of pulse-like records. It is seen that, for the 2-story steel frame structure, the pulse-like records with $T_p/T_1>1$ produce higher MIDRs than the non-pulse-like records. When the structure undergoes large deformation, the pulse-like records with large $T_p$ tend to coincide with the elongated period of the structure, resulting in increased responses. In the case of 9-story structure, the records with $1<T_p/T_1<2$ produce lower drift values than the non-pulse-like records, whereas the records having $T_p/T_1>2$ and $T_p/T_1<1$ produce larger responses than the non-pulse-like records. These results indicate that the $T_p/T_1$ is not always a good proxy to characterize the damaging potential of the pulse-like ground motions because the aggressive or benign behavior of the velocity pulses may change depending on the structural characteristics and the ground-motion intensity level.

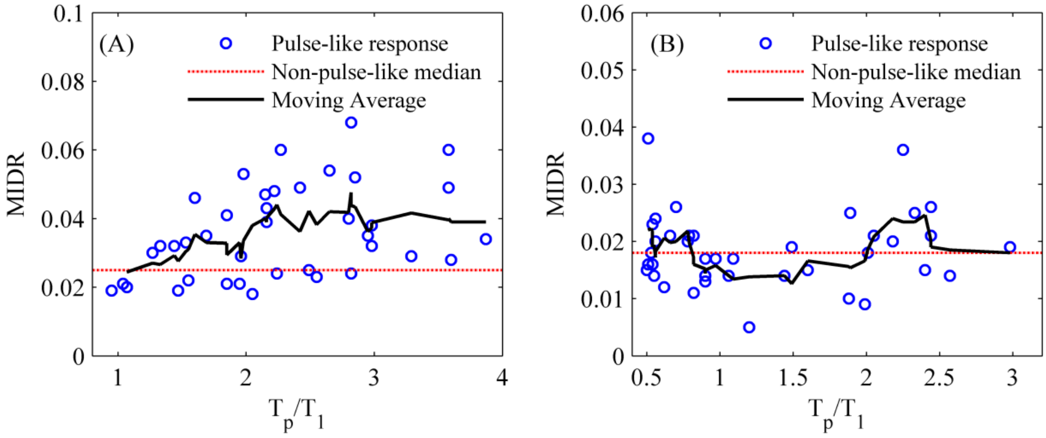


Fig. 6 – Dependence of MIDRs on $T_p/T_1$ for the (A) 2- story and (B) 9-story steel-frame structures. The horizontal line indicates the median response of the non-pulse-like record set [6].

## 6. Efficiency and Sufficiency of the IP($T_1$)

The results of the previous sections suggest that the pulse period is not always a good proxy for the damaging effect of pulse-like records. We find that the proposed [Sa($T_1$), IP($T_1$)] vector IM gives a better representation of the damage potential of the near-fault ground motions than using the [Sa($T_1$), velocity pulse, $T_p$] vector IM. This section evaluates the ability of the IP($T_1$) to capture the damage potential of near-fault ground motions. Fig. 7 illustrates the relationship between the IP($T_1$) and MIDR for the ground motions that are scaled to the same Sa($T_1$) level. The $R^2$ statistics for the 2- and 9-story steel-frame structures (based on regression fits using the pooled pulse-like and non-pulse-like subsets) are 0.57 and 0.53, respectively. The results show that the IP($T_1$) explains a large proportion of variance in MIDR and has a large effect on nonlinear structural response. Fig. 7 also shows the linear fits to the pulse-like and non-pulse-like records. We repeat the regression using the dummy (or indicator) variable for the pulse-like and non-pulse-like records in order to determine whether the functional relationship between IP($T_1$) and MIDR is same for both record sets. The F-test statistics [11] showed that the coefficients of the dummy variables are statistically insignificant ($p>0.05$), indicating that the responses obtained from pulse-like and non-pulse-like records are statistically equivalent. This also shows that it is not necessary to distinguish between pulse-like and non-pulse-like records when estimating the seismic demand based on IP($T_1$).

The conditional standard deviation of the residuals of the linear regression fit ($\sigma_{lnMIDR}$) can be used to quantify the efficiency of the vector-IM. The mean and standard deviation of ln(MIDR) can be computed as follows:

$$\mu_{lnMIDR}(IP(T_1)) = \beta_0 + \beta_1 \ln(IP(T_1)) \tag{3}$$

$$\sigma_{lnMIDR} = \sqrt{\frac{\sum_{i=1}^{n}(lnMIDR_i - \mu_{lnMIDR}(IP(T_1))^2}{n-2}} \tag{4}$$

where $\beta_0$ and $\beta_1$ are parameters of linear regression, $lnMIDR_i$ is the natural logarithm of the MIDR corresponding to the $i^{th}$ record, and $n$ is defined as the number of ground-motion records. Assuming that the MIDR at a given intensity level is lognormally distributed, the logarithmic standard deviations of the drift values obtained from Sa($T_1$) for the 2- and 9-story steel-frame structures are 0.42 and 0.31 natural log units, respectively. After incorporating the effect of IP($T_1$), the dispersions in the MIDRs for the 2- and 9-story steel-frame buildings are obtained as 0.25 and 0.21 natural log units, respectively, indicating that the vector IM leads to an average 35% reduction in the standard deviation compared to the case in which only Sa($T_1$) is used. We interpret the results as suggesting that the consideration of the IP($T_1$) in ground-motion selection would help reduce the number of records to be used in nonlinear dynamic analysis.

We next check the sufficiency of the IP($T_1$) with respect to pulse period by comparing the estimated MIDR at the 2/50 seismic hazard levels based on Sa($T_1$) alone with those based on the [Sa($T_1$), IP($T_1$)] vector IM. The left panel of Fig. 8 shows the residuals obtained using the Sa($T_1$) versus $T_p/T_1$ for the 2- and 9-story steel-frame structures, respectively. The residuals obtained after regressing the structural response against the IP($T_1$) are shown in the right panel of Fig.8. We evaluate the sufficiency by quantifying the area under the moving-average curve [5]. Note that if the vector IM is sufficient with respect to $T_p$, there should be no trend with $T_p$. As is evident from Fig. 8, the inclusion of the IP($T_1$) leads to a reduction in the area under the moving average curve and removes the trend in the residuals. The area reduction percentages for the 2- and 9-story steel-frame buildings are 55% and 40%, respectively. Further, the standard deviation of the residuals is reduced by approximately 35% in both cases. The results indicate that the use of the vector IM consisting of Sa($T_1$) and IP($T_1$) accounts for the pulse period effects on structural responses and eliminates the sensitivity of the drift responses to the presence of the velocity pulses in near-fault ground motions. These results also indicate that there is no need for a detailed record selection when assessing the structural response based on IP($T_1$).

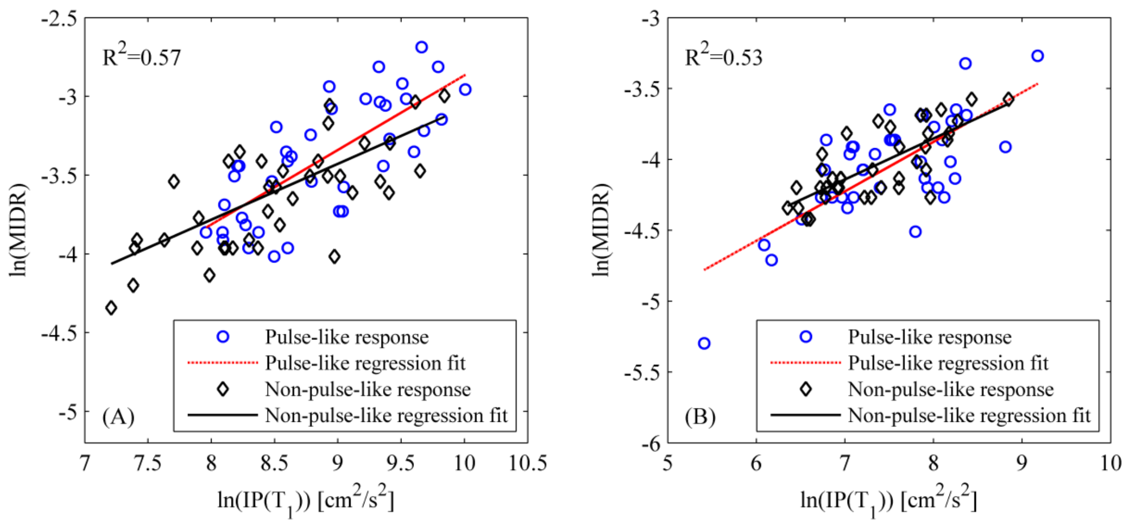


Fig. 7 – Relationships between Instantaneous Powers (IPs) and MIDRs of the (A) 2- and (B) 9-story steel-frame structures. The sets of pulse-like and non-pulse-like records are conditioned on the target Sa($T_1$) levels. $R^2$ statistics are based on regression fits to the pooled data [6].



 

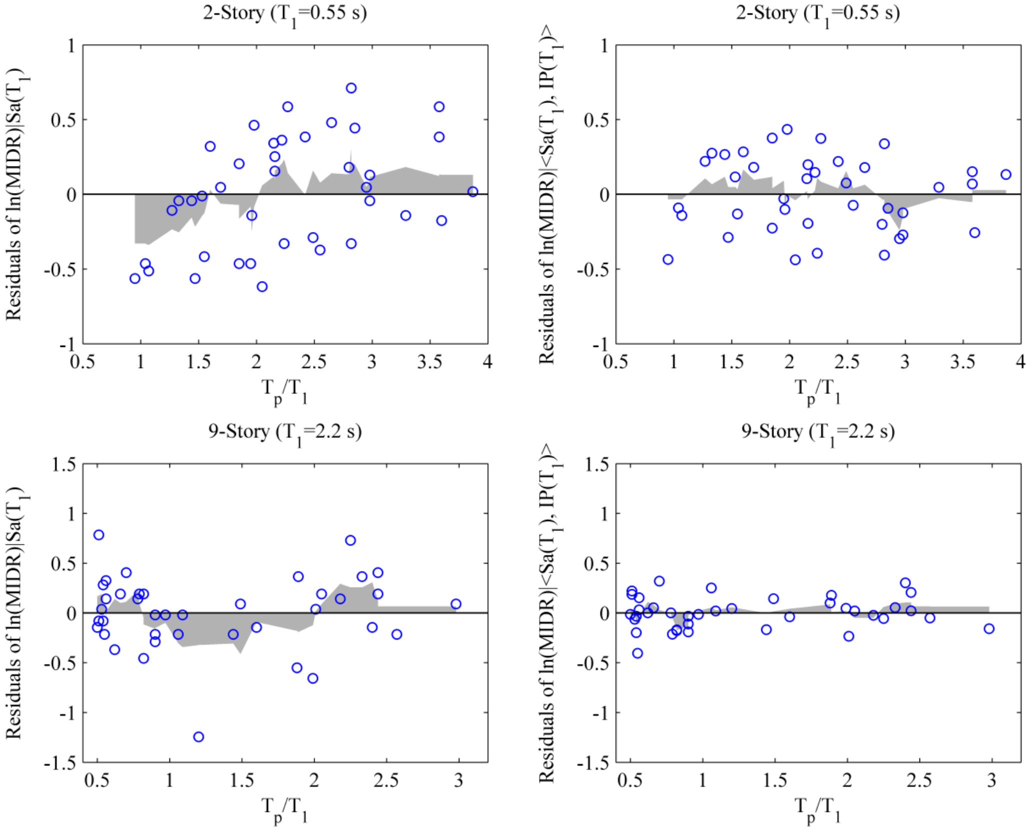


Fig. 8 – Residuals of In(MIDR) versus $T_p/T_1$ when the predictions based on $Sa(T_1)$ (left panel) and [$Sa(T_1)$, $IP(T_1)$] (right panel) for the 2- and 9-story steel-frame structures, at the 2/50 seismic hazard levels. Shaded areas represent the bias [6].

## 7. Comparisons of the Seismic Drift Hazard Curves

For a scalar IM, the annual rate of exceeding a given engineering demand parameter (EDP) level $x$ ($\lambda_{EDP}(x)$), that is, the seismic drift hazard curve, can be computed as follows:

$$\lambda_{EDP}(x) = \int_0^{\infty} P(EDP > x|IM = im) \left|\frac{d\lambda(im)}{d(im)}\right| d(im) \tag{5}$$

where $P(EDP > x|IM = im)$ is the conditional probability of exceeding an EDP value given the IM level, and $d\lambda(im)/d(im)$ is the slope of the site-specific annual rate of exceedance for the IM (i.e. the scalar hazard).

For the [$Sa(T_1)$, $IP(T_1)$] vector IM, the $\lambda_{EDP}(x)$ is computed by convolving the fragility surfaces with the site-specific seismic hazard curve given in terms of rate of exceedance:

$$\lambda_{EDP}(x) = \int_{im_1}\int_{im_2} P(EDP > x|Sa(T_1) = im_1, IP(T_1) = im_2) \left|\frac{\partial^2 \lambda(im_1,im_2)}{\partial(im_1)\,\partial(im_2)}\right| dim_2 dim_1 \tag{6}$$

where $\lambda(im_1, im_2)$ is the vector hazard for $Sa(T_1)$ and $IP(T_1)$. To compute the vector hazard for $Sa(T_1)$ and $IP(T_1)$, we use the conditional ground-motion model for $IP(T_1)$ developed by Zengin and Abrahamson [12].

The functional form is given by:



 

$$\ln(IP(T_1)) = a_1 + a_2 \ln\big(Sa(T_1)\big) + a_3(M-6) + a_4 \ln\big(R_{rup} + 5\exp(0.4(M-6))\big) \quad (7)$$

where $IP(T_1)$ is in $cm^2/s^2$, $R_{rup}$ is the rupture distance in km, M is the moment magnitude, and $Sa(T_1)$ is the 5% damped elastic spectral acceleration in g, $a_1$, $a_2$, $a_3$, and $a_4$ are the coefficients of the model. The details of the vector hazard computation can be found in [6].

Fig. 9 illustrates the seismic drift hazard curves computed using the scalar IM and the vector IM for the structures examined here. As can be seen, the rates of exceeding the MIDRs estimated using $Sa(T_1)$ are higher than those produced using the [$Sa(T_1)$, $IP(T_1)$] vector IM for both structures. Here, the rate of exceedance of a drift value of 0.10 represents the collapse risk of structure. It is seen that the collapse risk estimated using $Sa(T_1)$ is higher than those obtained using the vector IM. In the case of $Sa(T_1)$, the IP values of the records are not checked and the median $IP(T_1)$ may be biased high or low depending on the records utilized in this study. Our results show that the distribution of the structural response given $Sa(T_1)$ is affected by the $IP(T_1)$ values of the records. Thus, if the distribution of the $IP(T_1)$ values of the record set does not match with the target distribution obtained from the conditional ground-motion model for $IP(T_1)$, the collapse risk estimated using scalar IM (i.e., $Sa(T_1)$) may be biased. For example, the median $IP(T_1)$ values of the records at the 2/50 seismic hazard levels for the 2- and 9-story steel structures are 5983 and 1700, respectively, whereas the median IPs for the 2- and 9-story structures obtained using conditional ground-motion model are 3221 and 1237, respectively. These results suggest that the high $IP(T_1)$ values of the scaled subsets lead to an overestimation of the drift hazard estimates if scalar hazard is used. If $Sa(T_1)$ is used as an IM, it is necessary to select the records based on the target distribution of $IP(T_1)$ at each $Sa(T_1)$ level obtained from the conditional ground-motion model for IP given in Eq. (7). An alternative approach is to perform the double integration for the vector IM, which reduces the dependence on the record selection and leads to reliable and accurate estimates of the drift hazard.

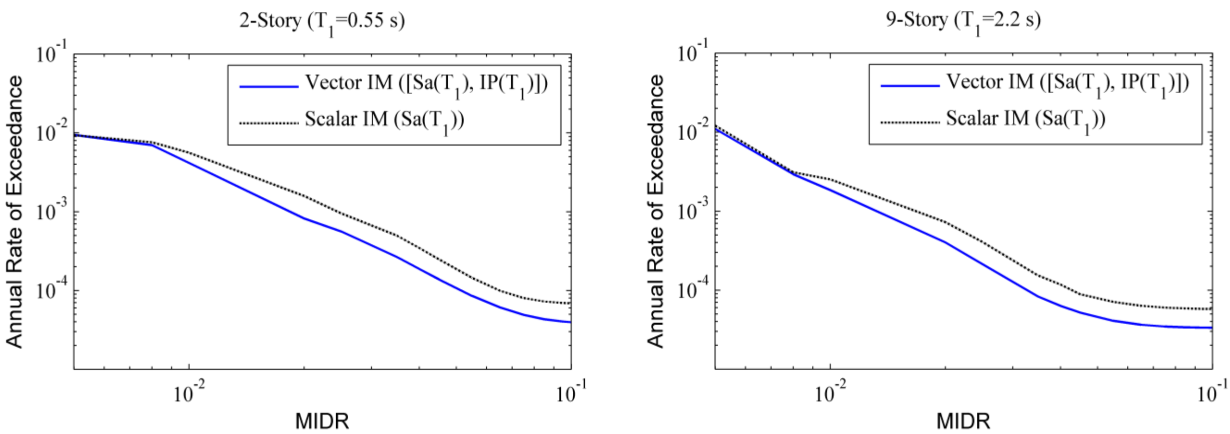


Fig. 9 – Comparisons of drift hazard curves using scalar and vector IM, for the 2- and 9-story steel-frame structures [6].

## 8. Conclusions

A new vector-valued IM ([$Sa(T_1)$, $IP(T_1)$]) is proposed to capture the damaging potential of the near-fault ground motions. In particular, we find that the $IP(T_1)$ values of the pulse-like and non-pulse-like records are highly correlated with the peak displacement-based structural responses of 2- and 9-story steel frame structures for the given $Sa(T_1)$ levels. Although the destructive effects of the pulse-like records are commonly attributed to the ratio of the pulse period to the fundamental period of the structure ($T_p/T_1$), our results suggest that the $T_p/T_1$ is not always a good predictor of structural response for pulse-like records, and that its effect depends on the structural characteristics and intensity levels. We demonstrate that the [$Sa(T_1)$, IP($T_1$)] vector IM is insensitive to the variations in the pulse periods, and therefore the selection of pulse-like records based on $T_p$ would be redundant. Since the IP($T_1$) is more effective than the velocity pulse parameters in predicting the structural response, the use of the [Sa($T_1$), IP($T_1$)] vector IM will lead to more reliable and accurate estimation of the structural performance. If Sa($T_1$) is used as an IM, the conditional ground-motion model for IP($T_1$) can be used to compute the target IP($T_1$) values of the record subset at each Sa($T_1$) level.

## 9. References

[1] Baker JW, Cornell CA (2006) Spectral shape, epsilon and record selection. *Earthquake Engineering & Structural Dynamics*, **35**(9), 1077-1095.

[2] Tothong P, Luco N (2007) Probabilistic seismic demand analysis using advanced ground motion intensity measures. *Earthquake Engineering & Structural Dynamics*, **36**(13): 1837-1860.

[3] Tothong P, Cornell CA (2008) Structural performance assessment under near-source pulse-like ground motions using advanced ground motion intensity measures. *Earthquake Engineering & Structural Dynamics*, **37**(7): 1013-1037.

[4] Luco N, Cornell CA (2007) Structure-specific scalar intensity measures for near-source and ordinary earthquake ground motions. *Earthquake Spectra*, **23**(2): 357-392.

[5] Baker JW, Cornell CA (2008) Vector-valued intensity measures for pulse-like near-fault ground motions. *Engineering Structures*, **30**(4): 1048-1057.

[6] Zengin E, Abrahamson NA (2020) A vector-valued intensity measure for near-fault ground motions. *Earthquake Engineering & Structural Dynamics*, https://doi.org/10.1002/eqe.3261.

[7] Shahi SK, Baker JW (2014) An efficient algorithm to identify strong velocity pulses in multicomponent ground motions. *Bulletin of the Seismological Society of America*, **104**(5), 2456-2466.

[8] Zengin E, Abrahamson NA, Kunnath S (2020) Isolating the effect of ground-motion duration on structural damage and collapse of steel frame buildings. *Earthquake Spectra* https://doi.org/10.1177/8755293019891720.

[9] Lignos DG, Krawinkler H (2010) Deterioration modeling of steel components in support of collapse prediction of steel moment frames under earthquake loading. *Journal of Structural Engineering,* **137**:1291-1302.

[10] Cohen J (1992) A power primer, *Psychological bulletin*, **112**: 155.

[11] Neter J, Kutner MH, Nachtsheim CJ, Wasserman W (1996) Applied linear statistical models, Chicago: Irwin, Vol.**4**, p.318.

[12] Zengin E, Abrahamson NA (2020) Ground motion model for damaging characteristics of near-fault ground motions based on Instantaneous Power, *to be submitted.*



 